315 The evaluation of potential DDI risks of these drugs appears to be further
316 complicated by the presence of multiple OATP2B1 substrate binding sites. It should be
317 noted that the H- and L-sites found in E_1S uptake are not always identical to the uptake
318 sites of other substrates, as can be seen in the report showing that GFJ inhibits
319 OATP2B1-mediated fexofenadine uptake through preferentially interacting with its
320 L-site, while inhibiting OATP2B1-mediated pravastatin uptake through selective
321 interactions with its H-site [20]. Therefore, even though our results show that SMV and
322 ASV have H-site inhibition preference for E_1S uptake, such preferential inhibition sites
323 can be either the H- or L-site depending on the substrate. Because the above GFJ-drug
324 interaction characteristics are believed to be related to clinical findings [14,20,26],
325 detailed characterization of substrate-dependent preferential inhibitory site of SMV and
326 ASV is considered to be important in the full evaluation of their potential DDI risks.
327 As for other DAAs examined in this study, TLV was found to be an L-site
328 specific co-incubation inhibitor, and its high $[I]_2/IC_{50(co)}$ value suggests that its potential
329 DDI risks with the OATP2B1 substrate cannot be ruled out. Our results also show that,
330 even though DCV, but not SOF, has a moderate effect on the OATP2B1 function, its *in*
331 *vivo* effects are still assumed to be marginal due to low predicted $[I]_2/IC_{50(co)}$ values.
332 This assumption appears to be consistent with recent findings that co-administered DCV
333 does not affect ASV pharmacokinetics in humans, even if ASV is found to be a substrate
334 of OATP2B1 [27,28].
335 Taken together, in line with reports showing that the AUC of aliskiren,
336 montelukast and fexofenadine are reduced when co-administered with
337 OATP2B1-inhibiting fruit juices [14-18], we suggest interpreting our results as a
338 recommendation to consider possible DDI occurrences between SMV or ASV and
339 primary OATP2B1 substrates. Furthermore, this attention will be also helpful in drug
340 development, assuming that the putative OATP2B1 substrates are incorporated into new
341 chemical entities.
342 Notwithstanding the above, it should be also noted that OATP2B1-mediated
343 DDI assessments of SMV or ASV might result in confounding observations. One reason
344 for this is related to the fact that OATP2B1 is expressed in the liver as well [29]. This
345 means that, even if plasma unbound concentrations of SMV and ASV are low, their
346 potential inhibitory effects on hepatic OATP2B1 cannot be fully ruled out. Such hepatic
347 OATP2B1 inhibition, if it occurs, could contribute to increased plasma concentration of
348 a victim drug, which seems to be the opposite of what occurs at the small intestine.
349 Another reason is that SMV and ASV may affect other transporter and enzyme
350 functions [the Sovriad and Sunvepra interview forms]. It is well known that OATP2B1

351 substrates can be also recognized by other transporters, as well as by metabolic enzymes,
352 and, therefore, the effects of SMV or ASV on such drug transporters and enzymes (e.g.
353 intestinal P-glycoprotein and CYP3A4) might compromise their suppressive effects on
354 OATP2B1-mediated victim drug absorption.
355 Accordingly, while this study focused solely on OATP2B1, careful
356 consideration into the involvement of other transporters/enzymes in DDIs of SMV or
357 ASV with OATP2B1 substrates will be necessary for full *in vivo* DDI evaluation and
358 characterization.
359 Finally, the potential mechanisms behind long-lasting pre-incubation OATP2B1
360 inhibitory effects of SMV and ASV are worth mentioning, even though they have yet to
361 be elucidated. Based on the finding that pre-incubation synergistically augments
362 co-incubation effects in SMV, they appear to be distinct from those responsible for
363 co-incubation inhibition. One possibility of such long-lasting pre-incubation OATP2B1
364 inhibitory effects is that, once after SMV or ASV enters the cells, they interact with
365 OATP2B1 at the cytosolic side. This was first suggested by Shitara et al. [30], who
366 examined the long-lasting pre-incubation effects of cyclosporine A on the OATP1B1
367 and OATP1B3 functions in HEK293 and MDCK II cells.
368 However, it should be noted that we could not rule out the possibility that
369 non-specific binding plays roles in the pre-incubation effects. More specifically, it is
370 possible that pre-incubation with SMV or ASV might actually saturate non-specific
371 binding sites of OATP2B1, thereby allowing for an apparent reduction in their IC_{50}
372 values.
373 Therefore, in future experimental efforts to clarify how SMV or ASV
374 long-lasting pre-incubation enhances their co-incubation inhibition effects on OATP2B1
375 function, it is recommended that the above possibilities be taken into consideration. In
376 addition, detailed characterization of OATP2B1 inhibition types by SMV and ASV
377 (which currently remain elusive) may provide valuable clues for understanding those
378 inhibition mechanisms.
379 In conclusion, our results have demonstrated that SMV and ASV are new and
380 potent co-incubation, as well as long-lasting pre-incubation, inhibitors of OATP2B1 at
381 two active sites tested. These findings also indicate that SMV and ASV have potential
382 DDI risks with OATP2B1 substrate drugs, even though their likelihood and clinical
383 significance must be investigated by *in vivo* experiments in the future. In the interim,
384 however, cautions related to the DDI risk of SMV and ASV with primary OATP2B1
385 substrates may be recommended prior to the accumulation of such clinical data. TLV
386 might also pose DDI risks, even though they appear to be much less significant. In

387 contrast, SOF and DCV may be used without such caution. Finally, we expect that our
388 findings will contribute to better clinical management of current as well as future
389 anti-HCV therapies.

390 Funding: This work is funded by a Ministry of Health, Labor and Welfare Grant-in-Aid
391 for Scientific Research (Emergency Research Project to Conquer Hepatitis), Japan.
392 Competing interests: None declared.
393 Ethical approval: Not required.
394

References

[1] Tsubota A, Furihata T, Matsumoto Y, Chiba K. Sustained and rapid virological responses in hepatitis C clinical trials. Clin Invest 2013;3:1-11.

[2] Shah N, Pierce T, Kowdley KV. Review of direct-acting antiviral agents for the treatment of chronic hepatitis C. Expert Opin Investig Drugs 2013;22:1107-21.

[3] Burger D, Back D, Buggisch P, Buti M, Craxí A, Foster G, et al. Clinical management of drug-drug interactions in HCV therapy: challenges and solutions. J Hepatol 2013;58:792-800.

[4] Kiser JJ, Burton JR Jr, Everson GT. Drug-drug interactions during antiviral therapy for chronic hepatitis C. Nat Rev Gastroenterol Hepatol 2013;10:596-606.

[5] Garg V, van Heeswijk R, Lee JE, Alves K, Nadkarni P, Luo X. Effect of telaprevir on the pharmacokinetics of cyclosporine and tacrolimus. Hepatology 2011;54:20-7.

[6] Lee JE, van Heeswijk R, Alves K, Smith F, Garg V. Effect of the hepatitis C virus protease inhibitor telaprevir on the pharmacokinetics of amlodipine and atorvastatin. Antimicrob Agents Chemother 2011;55:4569-74.

[7] Garg V, Chandorkar G, Farmer HF, Smith F, Alves K, van Heeswijk RP. Effect of telaprevir on the pharmacokinetics of midazolam and digoxin. J Clin Pharmacol 2012;52:1566-73.

[8] Kunze A, Huwyler J, Camenisch G, Gutmann H. Interaction of the antiviral drug telaprevir with renal and hepatic drug transporters. Biochem Pharmacol 2012;84:1096-102.

[9] Chu X, Cai X, Cui D, Tang C, Ghosal A, Chan G, et al. In vitro assessment of drug-drug interaction potential of boceprevir associated with drug metabolizing enzymes and transporters. Drug Metab Dispos 2013;41:668-81.

[10] Furihata T, Matsumoto S, Fu Z, Tsubota A, Sun Y, Matsumoto S, et al. Different interaction profiles of direct-acting anti-hepatitis C virus agents with human organic anion transporting polypeptides. Antimicrob Agents Chemother 2014;58:4555-64.

[11] Dolton MJ, Roufogalis BD, McLachlan AJ. Fruit juices as perpetrators of drug interactions: the role of organic anion-transporting polypeptides. Clin Pharmacol Ther 2012;92:622-30.

[12] Tamai I. Oral drug delivery utilizing intestinal OATP transporters. Adv Drug Deliv Rev 2012;64:508-14.

[13] Tamai I, Nakanishi T. OATP transporter-mediated drug absorption and interaction.

Curr Opin Pharmacol 2013;13:859-63.
[14] Dresser GK, Bailey DG, Leake BF, Schwarz UI, Dawson PA, Freeman DJ, et al. Fruit juices inhibit organic anion transporting polypeptide-mediated drug uptake to decrease the oral availability of fexofenadine. Clin Pharmacol Ther 2002;71:11-20.
[15] Tapaninen T, Neuvonen PJ, Niemi M. Grapefruit juice greatly reduces the plasma concentrations of the OATP2B1 and CYP3A4 substrate aliskiren. Clin Pharmacol Ther 2010;88:339-42.
[16] Imanaga J, Kotegawa T, Imai H, Tsutsumi K, Yoshizato T, Ohyama T, et al. The effects of the SLCO2B1 c.1457C > T polymorphism and apple juice on the pharmacokinetics of fexofenadine and midazolam in humans. Pharmacogenet Genomics 2011;21:84-93.
[17] Mougey EB, Lang JE, Wen X, Lima JJ. Effect of citrus juice and SLCO2B1 genotype on the pharmacokinetics of montelukast. J Clin Pharmacol 2011;51:751-60.
[18] Tapaninen T, Neuvonen PJ, Niemi M. Orange and apple juice greatly reduce the plasma concentrations of the OATP2B1 substrate aliskiren. Br J Clin Pharmacol 2011;71:718-26.
[19] Shirasaka Y, Mori T, Shichiri M, Nakanishi T, Tamai I. Functional pleiotropy of organic anion transporting polypeptide OATP2B1 due to multiple binding sites. Drug Metab Pharmacokinet 2012;27:360-64.
[20] Shirasaka Y, Mori T, Murata Y, Nakanishi T, Tamai I. Substrate- and Dose-Dependent Drug Interactions with Grapefruit Juice Caused by Multiple Binding Sites on OATP2B1. Pharm Res 2014;31:2035-43.
[21] Shirasaka Y, Shichiri M, Murata Y, Mori T, Nakanishi T, Tamai I. Long-lasting inhibitory effect of apple and orange juices, but not grapefruit juice, on OATP2B1-mediated drug absorption. Drug Metab Dispos 2013;41:615-21.
[22] Tweedie D, Polli JW, Berglund EG, Huang SM, Zhang L, Poirier A, et al; International Transporter Consortium. Transporter studies in drug development: experience to date and follow-up on decision trees from the International Transporter Consortium. Clin Pharmacol Ther 2013;94:113-25.
[23] Karlgren M, Vildhede A, Norinder U, Wisniewski JR, Kimoto E, Lai Y, et al. Classification of inhibitors of hepatic organic anion transporting polypeptides (OATPs): influence of protein expression on drug-drug interactions. J Med Chem 2012;55:4740-63.
[24] Schiller C, Fröhlich CP, Giessmann T, Siegmund W, Mönnikes H, Hosten N, et al. Intestinal fluid volumes and transit of dosage forms as assessed by magnetic

resonance imaging. Aliment Pharmacol Ther 2005;22:971-79.
[25] Suzuki K, Shitara Y, Fukuda K, Horie T. Long-lasting inhibition of the intestinal absorption of fexofenadine by cyclosporin A in rats. J Pharm Sci 2012;101:2606-15.
[26] Lilja JJ, Kivistö KT, Neuvonen PJ. Grapefruit juice increases serum concentrations of atorvastatin and has no effect on pravastatin. Clin Pharmacol Ther 1999;66:118-27.
[27] Eley T, Sevinsky H, Huang SP, He B, Zhu K, Kandoussi H, et al. The pharmacokinetics of daclatasvir and asunaprevir administered in combination in studies in healthy subjects and patients infected with hepatitis C virus. Clin Drug Investig 2014;34:661-71.
[28] Eley T, Han YH, Huang SP, He B, Li W, Bedford W, et al. Organic anion transporting polypeptide-mediated transport of, and inhibition by, asunaprevir, an inhibitor of hepatitis C virus NS3 protease. Clin Pharmacol Ther 2015;97:159-66.
[29] Kullak-Ublick GA, Ismair MG, Stieger B, Landmann L, Huber R, Pizzagalli F, et al. Organic anion-transporting polypeptide B (OATP-B) and its functional comparison with three other OATPs of human liver. Gastroenterology 2001;120:525-33.
[30] Shitara Y, Takeuchi K, Nagamatsu Y, Wada S, Sugiyama Y, Horie T. Long-lasting inhibitory effects of cyclosporin A, but not tacrolimus, on OATP1B1- and OATP1B3-mediated uptake. Drug Metab Pharmacokinet 2012;27:368-78.

Tables

Table 1. The $IC_{50(co)}$ values of DAAs on E_1S transport through the H- and L-sites of OATP2B1 (a co-incubation inhibition method)

DAA	$IC_{50(co)}$ (μM)	
	H-site	L-site
TLV	N/A[a]	16.22 ± 2.73
SMV	0.49 ± 0.12	10.15 ± 2.80
ASV	0.16 ± 0.06	0.92 ± 0.08
DCV	N/D[b]	N/D[b]
SOF	N/A[a]	N/A[a]

[a], not available due to lack of inhibition effects.

[b], not determined because the values did not fit with the inhibition curve. If the values were tentatively calculated, they were 35.5 ± 4.10 and 50.10 ± 18.02 (μM) for the H- and L-sites, respectively.

Table 2. The enhancement effects of long-lasting SMV or ASV pre-incubation on their co-incubation inhibition potency against E_1S uptake through the H- and L-sites of OATP2B1

DAA	Affinity site	$IC_{50(co\&pre)}$[a] (μM)	$IC_{50(co)}/IC_{50(co\&pre)}$[b]
SMV	H-site	0.19 ± 0.05*	2.6
	L-site	0.50 ± 0.07**	20.3
ASV	H-site	0.08 ± 0.01	2.0
	L-site	0.34 ± 0.11**	2.7

[a], $IC_{50(co\&pre)}$ is the IC_{50} value of SMV or ASV on E_1S transport through the H- and L-sites of OATP2B1, which is determined by a pre- and co-incubation inhibition method. The single and double asterisks indicate that the value is significantly different ($p < 0.05$ and $p < 0.005$, respectively) from the corresponding $IC_{50(co)}$ value (Table 1) in the statistical analysis.

[b], $IC_{50(co)}/IC_{50(co\&pre)}$ indicates the ratio of the IC_{50} obtained by co-incubation to that obtained by pre- and co-incubation.

Table 3. *In vitro* evaluation of SMV and ASV DDI potential based on their inhibition properties toward the H- and L-sites of OATP2B1

DAA	Dose	MW	$[I]_2$ [a]	H-site		L-site	
	mg	g/mol	μM	$[I]_2/IC_{50(co)}$	$[I]_2/IC_{50(co\&pre)}$	$[I]_2/IC_{50(co)}$	$[I]_2/IC_{50(co\&pre)}$
SMV	150	749.9	800	1,632	4,211	78.8	1,600
ASV	100	748.3	535	3,344	6,688	582	1,574

[a], $[I]_2$ is the theoretical maximal gastrointestinal DAA concentration after its oral administration calculated as the clinical dose (mg) in a volume of 250 mL.

Figure captions

Fig. 1. Functional expression of OATP2B1 in 2B1/HEK cells.

A. OATP2B1 mRNA expression in 2B1/HEK was examined using RT-PCR. GAPDH mRNA expression was used as an internal control. B. OATP2B1 protein expression in 2B1/HEK cells was confirmed by Western blotting. Na^+/K^+ ATPase was used for a plasma membrane marker. C. E_1S (0.005 or 50 μM) transport mediated by the H- or L-site of OATP2B1 was measured in the presence or absence of a typical H- or L-site inhibitor, respectively. TCA (1 mM) is an inhibitor preferentially acting on the H-site, and TST (1 mM) is a specific inhibitor for the L-site, while BSP (100 μM) inhibits both affinity sites. Each value represents the mean ± S.D. of three independent determinations, each conducted in duplicate.

Fig. 2. Co-incubation inhibitory effects of DAA on E_1S transport mediated by the H- and L-sites of OATP2B1.

Uptake of E_1S (0.005 and 50 μM) through the H- or L-site of OATP2B1 (closed and open circles, respectively) was measured in the presence of a DAA. The DAA concentrations were from 0.01 to 100 μM and the uptake level was determined by subtracting the uptake level of mock/HEK from that of 2B1/HEK. The results were shown as percentages of uptake level relative to that of the DMSO (0.1%)-treated cells (= 100%). Each value represents the mean ± S.D. of three independent determinations, each conducted in duplicate.

Fig. 3. Effects of pre-incubation with DAA on E_1S uptake through the H- and L-sites of OATP2B1.

After 2B1/HEK were pre-incubated with DAA for one hour, E_1S uptake mediated by the H- or L-site of OATP2B1 was measured in the absence of the DAA (closed and open circles, respectively). The uptake level was determined by subtracting the uptake level of mock/HEK from that of 2B1/HEK. Data were shown as percentages of the uptake level relative to that of the DMSO (0.1%) pre-treated cells (= 100%). Each value represents the mean ± S.D. of three determinations, each conducted in duplicate.

Fig. 4. Long-lasting pre-incubation inhibitory effects of SMV or ASV on E_1S uptake

566 through the H- and L-sites of OATP2B1.
567
568 Immediately after pre-incubation with SMV or ASV (1.0 μM) for one hour, 2B1/HEK
569 were further incubated for 0, 1 or 3 hours with DAA-free fresh culture medium. Then,
570 E_1S uptake mediated by the H- or L-site of OATP2B1 was measured in the absence of
571 the DAA (closed and open circles, respectively). The uptake level was determined by
572 subtracting the uptake level of mock/HEK from that of 2B1/HEK. Data were shown as
573 percentages of uptake level relative to that of the DMSO (0.1%) pre-treated cells (=
574 100%). Each value represents the mean ± S.D. of three determinations, each conducted
575 in duplicate.
576
577 Fig. 5. Enhancement effects of SMV and ASV pre-incubation on E_1S uptake through the
578 H- or L-site of OATP2B1.
579
580 Immediately after one hour pre-incubation with SMV or ASV, E1S uptake mediated by
581 the H- or L-site of OATP2B1 was measured in the presence of SMV or ASV (closed
582 circles). The concentration of a DAA ranged from 0.001 to 10 μM for SMV and from
583 0.001 to 1 μM for ASV. The dashed lines indicate the fitting curves of SMV and ASV
584 co-incubation inhibition effects on E_1S uptake (Fig.1), which are shown for comparison.
585 The uptake level was determined by subtracting the uptake level of mock/HEK from
586 that of 2B1/HEK. The results were shown as percentages of uptake level relative to that
587 of the DMSO (0.1%)-treated cells (= 100%). Each value represents the mean ± S.D. of
588 three independent determinations, each conducted in duplicate.

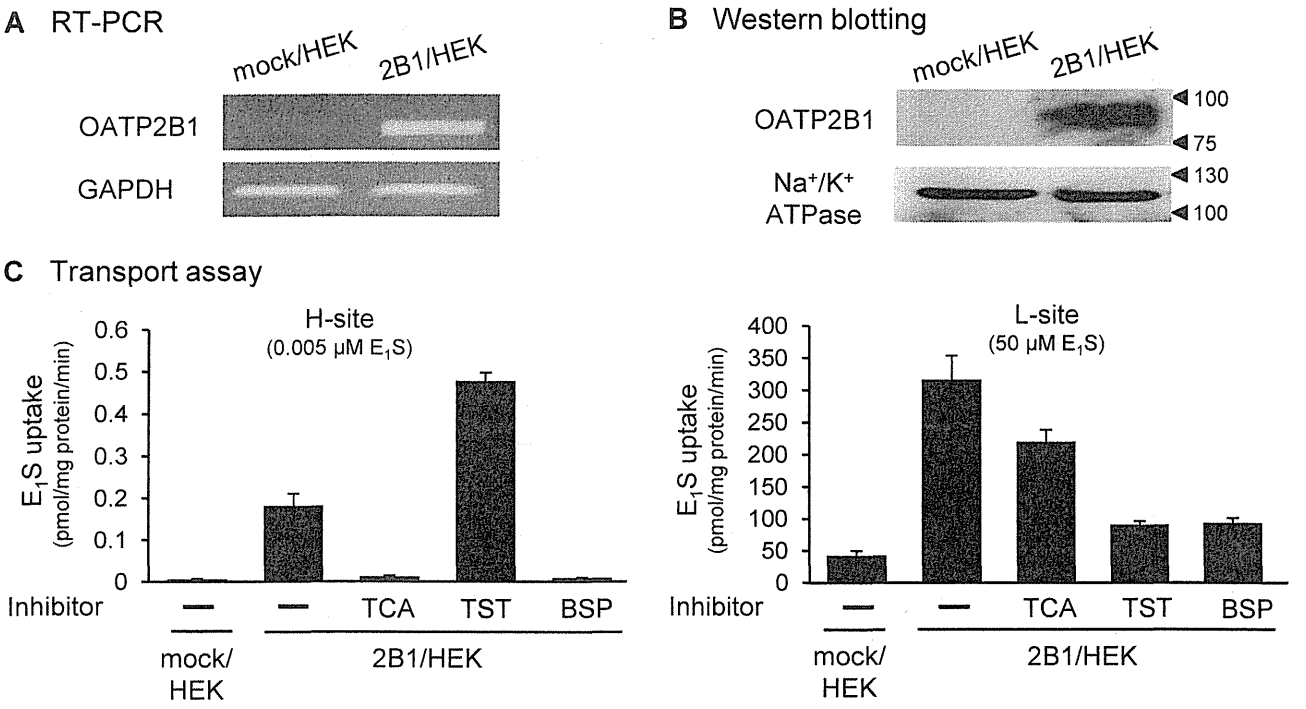

Fig. 1. Functional expression of OATP2B1 in 2B1/HEK cells.

A. OATP2B1 mRNA expression in 2B1/HEK was examined using RT-PCR. GAPDH mRNA expression was used as an internal control.
B. OATP2B1 protein expression in 2B1/HEK cells was confirmed by Western blotting. Na^+/K^+ ATPase was used for a plasma membrane marker.
C. E_1S (0.005 μM or 50 μM) transport mediated by the H- or L-site of OATP2B1 was measured in the presence or absence of a typical H- or L-site inhibitor, respectively. TCA (1 mM) is an inhibitor preferentially acting on the H-site, and TST (1 mM) is a specific inhibitor for the L-site, while BSP (100 μM) inhibits both affinity sites. Each value represents the mean ± S.D. of three independent determinations, each conducted in duplicate.

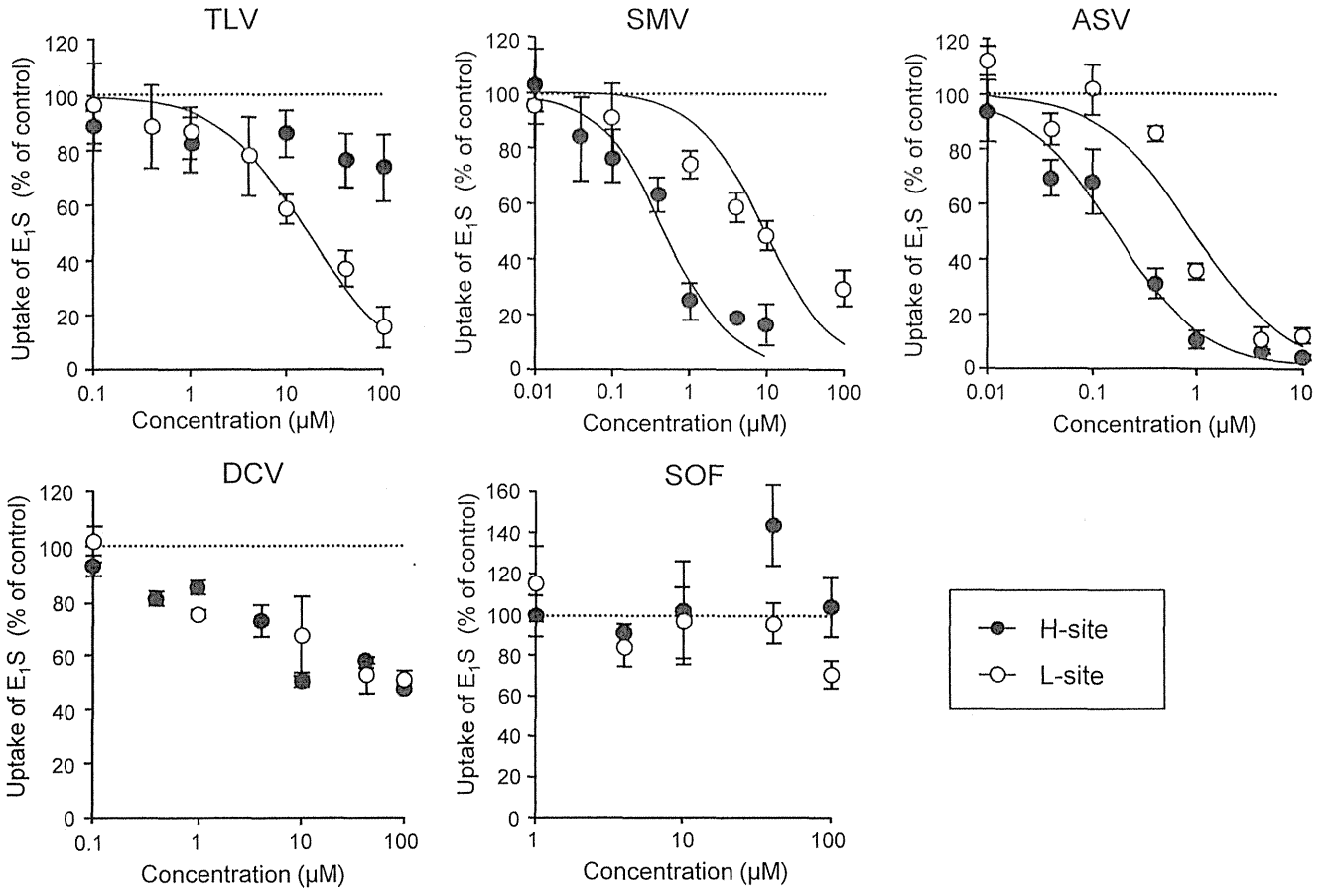

Fig. 2. Co-incubation inhibitory effects of DAA on E_1S transport mediated by the H- and L-sites of OATP2B1.

Uptake of E_1S (0.005 and 50 μM) through the H- or L-sites of OATP2B1 (closed and open circles, respectively) was measured in the presence of a DAA. The DAA concentrations were from 0.01 to 100 μM and the uptake level was determined by subtracting the uptake level of mock/HEK from that of 2B1/HEK. The results were shown as percentages of uptake level relative to that of the DMSO-treated cells (100%). Each value represents the mean ± S.D. of three independent determinations, each conducted in duplicate.

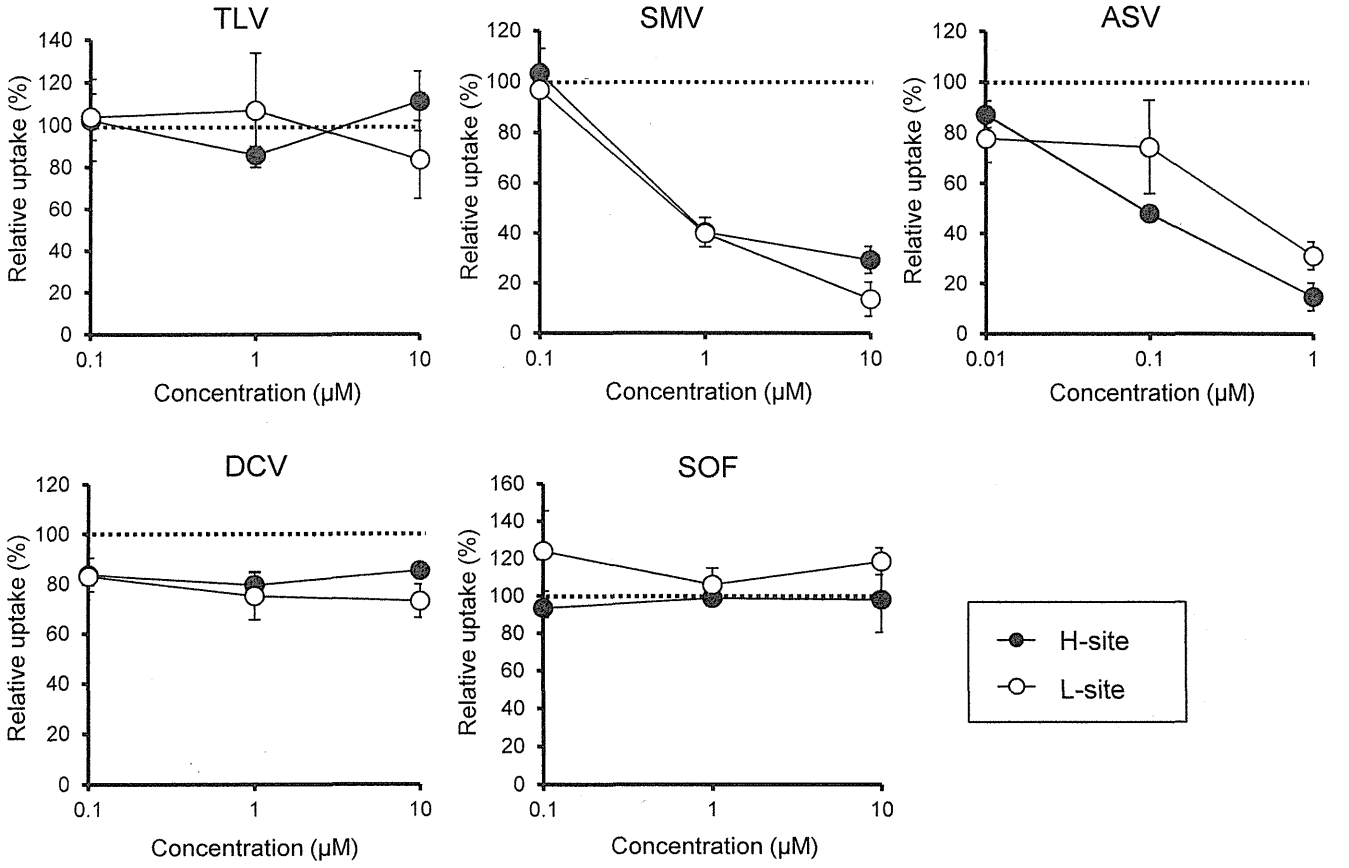

Fig. 3. Effects of pre-incubation with DAA on E_1S uptake through the H- and L-sites of OATP2B1.

After 2B1/HEK were pre-incubated with DAA for one hour, E_1S uptake mediated by the H- or L-site of OATP2B1 was measured in the absence of the DAA (closed and open circles, respectively). The uptake level was determined by subtracting the uptake level of mock/HEK from that of 2B1/HEK. Data were shown as percentages of the uptake level relative to that of the DMSO (0.1%) pre-treated cells (100%). Each value represents the mean ± S.D. of three determinations, each conducted in duplicate.

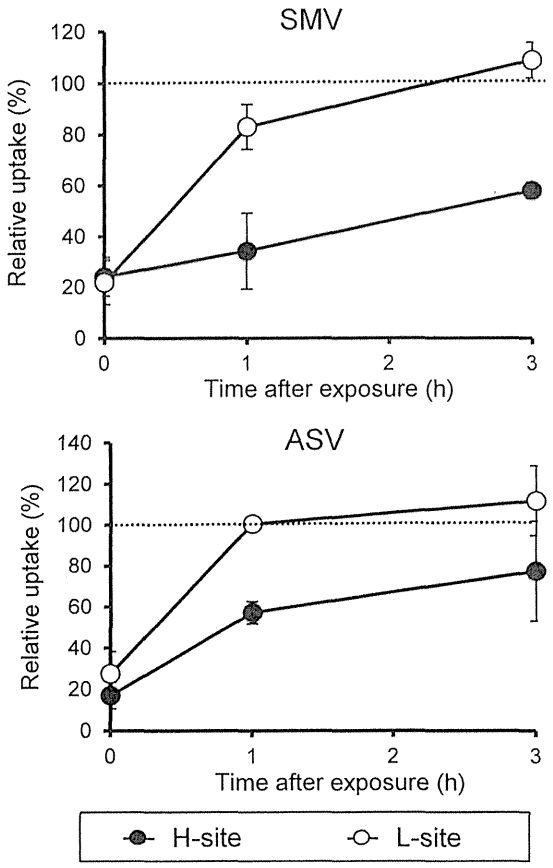

Fig. 4. Long-lasting pre-incubation inhibitory effects of SMV or ASV on E_1S uptake through the H- and L-sites of OATP2B1.

Immediately after pre-incubation with SMV or ASV (1.0 μM) for one hour, 2B1/HEK were further incubated for 0, 1 or 3 hours with DAA-free fresh culture medium. Then, E_1S uptake mediated by the H- or L-site of OATP2B1 was measured in the absence of the DAA (closed and open circles, respectively). The uptake level was determined by subtracting the uptake level of mock/HEK from that of 2B1/HEK. Data were shown as percentages of uptake level relative to that of the DMSO (0.1%) pre-treated cells (100%). Each value represents the mean ± S.D. of three determinations, each conducted in duplicate.

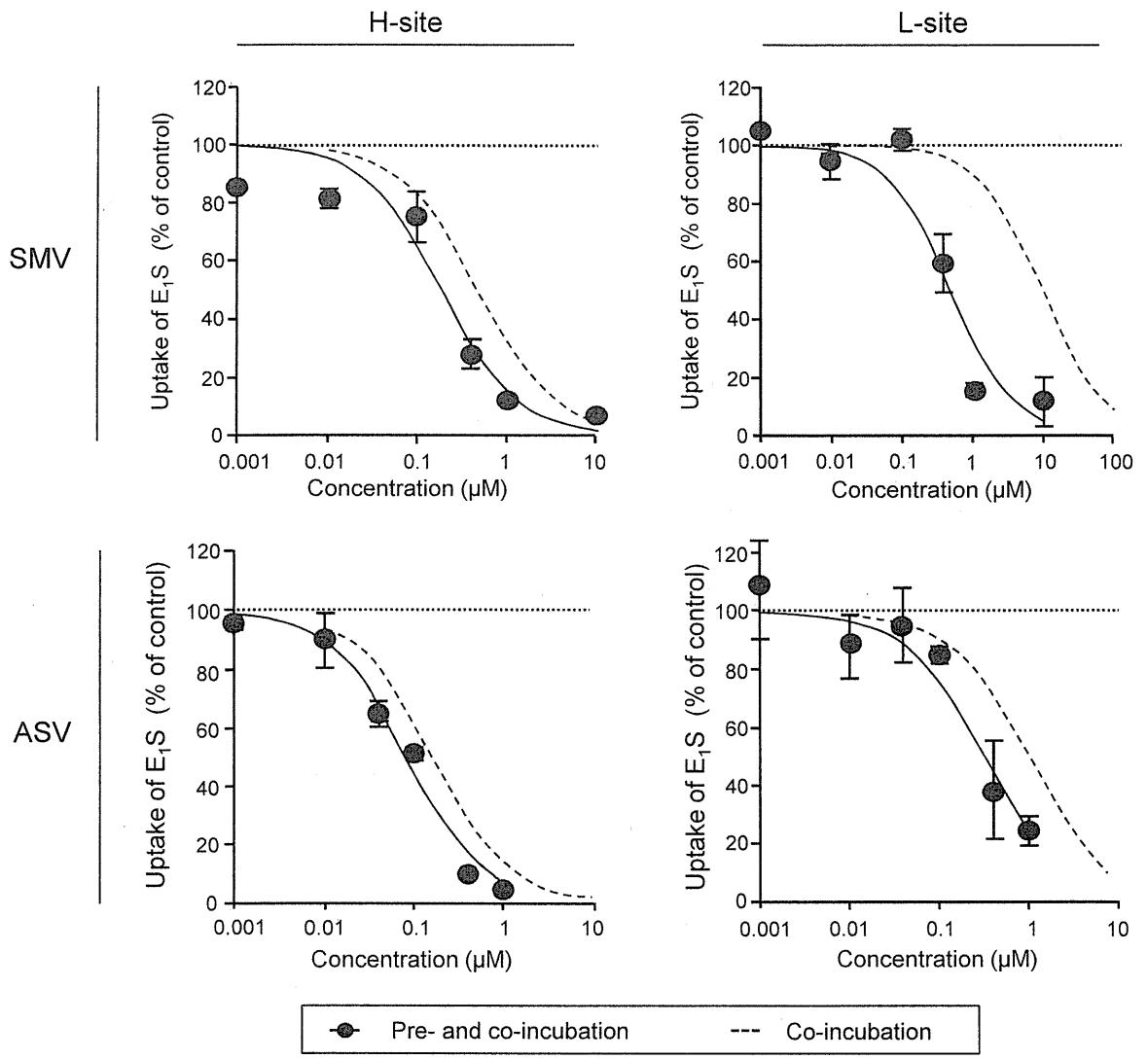

Fig. 5. Enhancement effects of SMV and ASV pre-incubation on E_1S uptake through the H- or L-site of OATP2B1.

Immediately after one hour pre-incubation with SMV or ASV, E_1S uptake mediated by the H- or L-site of OATP2B1 was measured in the presence of SMV or ASV (closed circles). The concentration of a DAA ranged from 0.001 to 10 μM for SMV and from 0.001 to 1 μM for ASV. The dashed lines indicate the fitting curves of SMV and ASV co-incubation inhibition effects on E_1S uptake (Fig.1), which are shown for comparison. The uptake level was determined by subtracting the uptake level of mock/HEK from that of 2B1/HEK. The results were shown as percentages of uptake level relative to that of the DMSO-treated cells (100%). Each value represents the mean ± S.D. of three independent determinations, each conducted in duplicate.

AAC
Journals.ASM.org

Different Interaction Profiles of Direct-Acting Anti-Hepatitis C Virus Agents with Human Organic Anion Transporting Polypeptides

Tomomi Furihata,[a] Shogo Matsumoto,[a] Zhongguo Fu,[a] Akihito Tsubota,[b] Yuchen Sun,[a] Sayaka Matsumoto,[a] Kaoru Kobayashi,[a] Kan Chiba[a]

Laboratory of Pharmacology and Toxicology, Graduate School of Pharmaceutical Sciences, Chiba University, Chiba-shi, Chiba, Japan[a]; Institute of Clinical Medicine and Research, Jikei University School of Medicine, Kashiwa-shi, Chiba, Japan[b]

Simeprevir (SMV), asunaprevir (ASV), daclatasvir (DCV), and sofosbuvir (SFV), which are newly developed direct-acting antiviral agents (DAAs) against hepatitis C virus (HCV) infection, are among the key components of anti-HCV regimens. Preclinical studies have identified inhibitory properties for some of these DAAs against organic anion transporting polypeptide 1B (OATP1B) functions. However, their details remain mostly uncharacterized. Because OATP1B1 and OATP1B3 play determinant roles in the pharmacokinetics of various drugs via their uptake into human hepatocytes, it is plausible that the inhibition of these OATP1Bs by a DAA would create a potential risk of drug-drug interaction, which has been an emerging concern in anti-HCV therapy. Accordingly, in the present study, we intended to clarify the inhibitory characteristics of newly developed DAAs toward OATP1B1 and -1B3 functions. The results of our coincubation inhibition assays have shown that all tested DAAs could inhibit OATP1B1 functions and that SMV, ASV, and DCV (to a lesser extent), but not SFV, exhibited long-lasting preincubation inhibitory effects on OATP1B1 functions. It was also found that the preincubation inhibitory effects of SMV and ASV could augment their coincubation inhibition potency. Furthermore, significant, but differential, inhibitory effects of the DAAs on the OATP1B3 function were identified. To summarize, our results clearly show that the newly developed DAAs are newly identified OATP1B1 and OATP1B3 inhibitors with distinctive interaction properties. It is believed that these inhibition profiles will provide essential information to all concerned parties with respect to the clinical significance of DAA-mediated inhibition of OATP1Bs in anti-HCV therapy.

Direct-acting antiviral agents (DAAs) against hepatitis C virus (HCV) proteins have dramatically improved clinical outcomes in chronic hepatitis C therapy. Recent clinical studies have shown that addition of telaprevir (TLV) or boceprevir (BOC), which are the first nonstructural 3/4A (NS3/4A) protease inhibitors, to the combination therapy of pegylated alpha interferon and ribavirin significantly enhances the rate of a sustained virological response in up to approximately 80% of patients carrying the HCV genotype 1 (1, 2). In addition, even higher treatment efficacy can be expected with the introduction of newly developed DAAs, including the NS3/4 protease inhibitors simeprevir (SMV) and asunaprevir (ASV), the NS5A inhibitor daclatasvir (DCV), and the NS5B inhibitor sofosbuvir (SFV) (1). The significantly reduced toxic properties of these new DAAs in comparison with those of TLV and BOC have also been highlighted in clinical studies, which adds further value to the use of these new agents in anti-HCV therapy.

The high efficacy of TLV and BOC aside, it has become increasingly evident that there are clinically significant risks of drug-drug interaction (DDI) when DAAs are coprescribed with various drugs (3, 4). For example, it has been reported that TLV increased the area under the curve of atorvastatin, cyclosporine (CsA), and tacrolimus by 7.9-fold, 4.6-fold, and 70-fold, respectively (5, 6), and, consequently, precautions related to the coadministration of these drugs with TLV have been noted (Incivek prescribing information, Vertex Pharmaceuticals Inc., Cambridge, MA). Likewise, the DDI properties of BOC with numerous drugs have been shown previously although BOC interactions have occurred apparently to a lesser extent (3, 4). TLV and BOC are inhibitors of cytochrome P450 3A4 (CYP3A4) as well as organic anion transporting polypeptides (OATPs) (7–9), which play determinant roles in the pharmacokinetics of various drugs. Therefore, inhibition of these functions is considered likely to contribute to the aforementioned DDIs. Because a detrimental DDI often results in unintentional toxic effects of the victim drug due to its increased systemic exposure, addressing DDIs caused by DAAs can be seen as a key issue in anti-HCV therapy.

OATP1B1 and OATP1B3 (OATP1B1/1B3), which are members of the *SLCO* gene family, are drug transporters that are primarily expressed at the plasma membrane of human hepatocytes. It has been established that both OATP1B1 and OATP1B3 play determinant roles in the pharmacokinetics of various anionic amphipathic molecules via their uptake from the circulatory system. Therefore, these OATP1Bs have been acknowledged as pivotal targets of DDI study in drug development and/or clinical settings (e.g., reference 10). Although they show a certain level of redundancy in their substrate spectrum, each OATP1B has its own substrate preferences. For example, it has been reported that estradiol-17β-glucuronide (E_2G) and statins (such as pravastatin, atorvastatin, and rosuvastatin) are substrates of both OATPs, whereas estrone-3-sulfate and cholecystokinin octapeptide (CCK-8) are primarily transported by OATP1B1 and

Received 4 March 2014 Returned for modification 1 April 2014
Accepted 21 May 2014
Published ahead of print 27 May 2014
Address correspondence to Tomomi Furihata, tomomif@faculty.chiba-u.jp.
Copyright © 2014, American Society for Microbiology. All Rights Reserved.
doi:10.1128/AAC.02724-14

Downloaded from http://aac.asm.org/ on July 15, 2014 by Chiba University

OATP1B3, respectively. Both OATPs are also known as conjugated or unconjugated bilirubin uptake transporters (11, 12).

OATP1B1 (and likely OATP1B3 as well) can be considered important targets for DDI research efforts, as exemplified by the reports showing the significant contribution of these OATPs to the DDI occurring between cerivastatin and CsA (13). Interestingly, Amundsen et al. (14) have shown that, among OATP1B inhibitors, preincubation of CsA enhances its direct (coincubation) inhibition potency against OATP1B1 in a cell-based assay, while Shitara et al. (15) have shown that the preincubation effect lasts for some time. Thus, long-lasting preincubation inhibitory effects have emerged as important characteristics in the functional inhibition mechanisms of OATP1Bs. On the other hand, the functional inhibition of OATP1Bs is also believed to play an important role in hyperbilirubinemia induced by OATP1B inhibitors, such as rifamycin SV, CsA, and atazanavir (11). Further information about the roles of OATPs in DDIs and hyperbilirubinemia can be found elsewhere (10, 16, 17).

Considering the clinically important roles played by OATP1Bs, a more precise understanding of the inhibitory characteristics of each DAA against the OATP1Bs is necessary for better clinical management in DAA-based anti-HCV therapy. However, detailed interaction profiles between the newly developed DAAs and OATP1Bs remain uncharacterized. Therefore, in the present study, we intended to clarify the inhibition characteristics of SMV, ASV, DCV, and SFV toward OATP1B1 and OATP1B3 functions, while simultaneously comparing the results with those obtained from TLV in order to evaluate their clinical significance.

MATERIALS AND METHODS

OATP1B expression plasmids. The development procedure of the pcDNA3.1(−)Zeo plasmid (Life Technologies, Carlsbad, CA) carrying OATP1B1 cDNA (OATP1B1/pcDNA3.1) and the pcDNA3.1(−)Neo plasmid (Life Technologies) carrying OATP1B3 cDNA (OATP1B3/pcDNA3.1) has been described previously (18, 19).

Plasmid transfection into HEK293 cells. Human embryonic kidney 293 (HEK293) cells were obtained from the Human Science Company (Tokyo, Japan) and cultured in Dulbecco's modified Eagle's medium (DMEM) (Life Technologies) supplemented with 10% fetal bovine serum and antibiotics in 5% CO_2 at 37°C.

The development procedure for HEK293 cells stably expressing OATP1B1 (1B1/HEK) and the cells carrying empty plasmid (mock/HEK) has been described previously (18). The cells were grown in the presence of 300 μg/ml phleomycin D1 (Zeocin; Invivogen, San Diego, CA).

OATP1B3/pcDNA3.1 was transfected into HEK293 cells, and then cells showing resistance to 400 μg/ml G418 disulfate (Sigma, St. Louis, MO) were collected. Among the various cell clones that resulted from the colony individualization method, the one with the highest OATP1B3 level was isolated and used in this study (here referred to as 1B3/HEK).

Total RNA extraction, cDNA synthesis, and RT-PCR. Total RNA extraction and cDNA synthesis using the HEK293 cells were performed according to the conventional methods described previously (18). Reverse transcription-PCR (RT-PCR) was performed to detect expression of an OATP1B isoform in the corresponding cells with the primers CAACAGT ATGGTCAGCCTTCATCTAAGG (sense) and AATTTGGCAATTCCAA CGGTGTTC (antisense) for detection of OATP1B1, the primers AACTC TTTGTTCTCTGCAACAGGAGGT (sense) and CTATAGATAAGCCCA AGTAGACCCTTCCA (antisense) for detection of OATP1B3, and the primers AGCCACATCGCTCAGACAC (sense) and GCCCAATACGAC CAAATCC (antisense) for detection of glyceraldehyde-3-phosphate dehydrogenase (GAPDH).

Western blotting. Western blotting was performed essentially using the methods described in our previous paper (20). Briefly, whole-cell lysate prepared from 1B1/HEK, 1B3/HEK, or mock/HEK cells was centrifuged at 1,000 × *g* for 10 min at 4°C, and the supernatant was then subjected to ultracentrifugation (100,000 × *g* for 40 min at 4°C). The pellet was solubilized with Tris-sucrose-EDTA buffer containing 0.8% NP-40, 0.4% deoxycholic acid, and 0.08% sodium dodecyl sulfate (SDS), followed by a second ultracentrifugation (100,000× *g* for 40 min at 4°C). The supernatant (soluble membrane fraction) was mixed with the lysis buffer and then incubated for 30 min at 37°C. The proteins were separated by SDS-polyacrylamide gel electrophoresis, followed by transblotting onto a polyvinylidene difluoride membrane. Bovine serum albumin (BSA; 5%) or skim milk (5%) was used for membrane blocking of OATP1B1 or OATP1B3, respectively.

The primary antibodies used were rabbit anti-LST-1 IgG (500-fold dilution; Alpha Diagnostic International, San Antonio, TX), rabbit anti-SLCO1B3 IgG (1,000-fold dilution; Sigma), and mouse anti-Na^+/K^+ ATPase IgG (1,000-fold dilution; Sigma). The secondary antibodies used were horseradish peroxidase-conjugated goat anti-rabbit IgG (5,000-fold dilution; Sigma) and horseradish peroxidase-conjugated goat anti-mouse IgG (5,000-fold dilution; Abcam, Cambridge, United Kingdom). Immunocomplex was detected using chemiluminescence.

Immunocytochemistry. Immunocytochemistry was performed essentially using the methods described in our previous paper (18). Briefly, 1B1/HEK, 1B3/HEK, or mock/HEK cells were seeded on a collagen-coated coverslip. The cells were fixed and permeabilized with a BD Cytofix/Cytoperm kit (BD Bioscience, Franklin Lakes, NJ). BSA (3%) was used for blocking. The primary antibodies used were rabbit anti-LST-1 IgG (200-fold dilution) or rabbit anti-SLCO1B3 IgG (200-fold dilution). The secondary antibodies used were Alexa Fluor 488-conjugated donkey anti-rabbit IgG (200-fold dilution; Life Technologies). Immunofluorescence was analyzed using confocal laser scanning immunofluorescence microscopy (FluoView FV-500; Olympus, Tokyo, Japan).

Transporter inhibition assays (coincubation method). OATP activity level was determined in 1B1/HEK and 1B3/HEK cells based essentially on previously described transport assay methods (18). Briefly, 1 day after the cells were seeded, they were exposed to sodium butyrate (10 mM; Sigma) for 24 h, after which the transport assay was performed using E_2G (100 nM; Sigma) for OATP1B1 or CCK-8 (10 nM; Peptide Institute, Osaka, Japan) for OATP1B3. ^{3}H-labeled E_2G and CCK-8 were obtained from American Radiolabeled Chemicals (St. Louis, MO) and PerkinElmer Life Science (Boston, MA), respectively. The uptake period was set to 3 min for OATP1B1 and to 5 min for OATP1B3, based on the results of preliminary experiments examining the uptake level linearity. The OATP activity level was calculated by subtracting the value obtained from mock/HEK cells from the value obtained from 1B1/HEK or 1B3/HEK cells.

Inhibition assays for validation of OATP1B expression in each cell line were performed using well-known inhibitors, rifampin (RIF; Wako, Osaka, Japan) for OATP1B1 and bromosulfophthalein (BSP; Sigma) for OATP1B3. Transport assays were performed using each cell line with the specific substrate in the presence of RIF (10 μM), BSP (100 μM), or their vehicle (dimethyl sulfoxide [DMSO]).

TLV, SMV, ASV, DCV, and SFV were purchased from Shanghai Biochempartner (Shanghai, China), ChemScene, LLC (Monmouth Junction, NJ), AdooQ BioScience LLC (Irvine, CA), ChemScene, LLC, and Medchemexpress, LLC (Princeton, NJ), respectively, and dissolved in DMSO. Inhibition assays using these DAAs were performed based on the above-described method. The E_2G concentration was set to 100 nM, and CCK-8 concentration was set to 10 nM, levels that were far below the K_m values of E_2G uptake by OATP1B1 and CCK-8 uptake by OATP1B3 (8.3 and 3.8 μM, respectively) (21). Inhibitor concentrations are indicated in the figure legends. A concentration that inhibited OATP activity level by 50% (IC_{50}) was calculated using the following formula: control (%) = $100/(1 + I/IC_{50})$, where control (%) represents the transporter-mediated uptake in the presence of various inhibitor concentrations relative to that in the absence of inhibitor, and I represents the inhibitor concentration.

Downloaded from http://aac.asm.org/ on July 15, 2014 by Chiba University

TABLE 1 Pharmacokinetic parameters of DAAs in humans

DAA	Dose (mg)	MW (g/mol)	f_u	C_{max}[a] (μM [ng/ml])	$C_{max,u}$ (μM)[b]	$C_{in,max,u}$ (μM)
TLV	750	679.8	0.37	5.49 (3,732)	2.031	10.2
SMV	150	749.9	0.01	5.85 (4,390)	0.059	0.10
ASV	200	748.3	0.01	0.85 (639)	0.007	0.06
DCV	60	738.9	0.01	2.34 (1,726)	0.023	0.04
SFV	400	529.5	0.37	1.14 (603)	0.421	6.01

[a] C_{max} values were obtained from the following reports: Buti et al. (36) for TLV, Sovriad interview form (Janssen Pharmaceutical K. K., Tokyo, Japan) for SMV, Eley et al. (presented at the Seventh International Workshop on Clinical Pharmacology of Hepatitis Therapy, Cambridge, MA, 27 to 28 June 2012) for ASV, Herbst and Reddy (37) for DCV, and Lawitz et al. (38) for SFV.
[b] $C_{max,u} = C_{max} \times f_u$.

***R* value calculation of OATP1B inhibition.** The maximum potential of OATP1B-mediated DDI was estimated by calculating the *R* value (17, 22). The *R* value was obtained by the following formula: $R = 1 + [(f_u \times I_{in,max})/IC_{50}]$, where f_u represents the blood unbound fraction of the inhibitor, and $I_{in,max}$ represents the estimated maximum inhibitor concentration at the inlet to the liver. $I_{in,max}$ was estimated using the following formula: $I_{in,max} = I_{max} + [(F_a \times dose \times K_a)/Q_h]$, where I_{max} is the maximum plasma concentration of the inhibitor, F_a is the dose fraction of the inhibitor that is absorbed, K_a is the absorption rate constant of the inhibitor, and Q_h is the hepatic blood flow rate (1,500 ml/min) in humans. As shown in the literature (7), F_a was set at 1, K_a was set at 0.03 min^{-1}, and the blood-to-plasma concentration ratio was assumed to be 1 for $I_{in,max}$ estimation. Information related to the pharmacokinetic parameters of the DAAs used in this study are summarized in Table 1, in which C_{max}, $C_{max,u}$, and $C_{in,max,u}$ are equivalent to I_{max}, $I_{max,u}$ and $I_{in,max,u}$ (estimated maximum unbound inhibitor concentration at the inlet to the liver), respectively.

Transporter inhibition assays (preincubation method). Based on the method described in a previous report (15), the 1B1/HEK, 1B3/HEK, or mock/HEK cells were preincubated with a DAA for 30 min at 0.1, 1.0, and 10 μM, after which the cells were washed twice with inhibitor-free transport assay buffer (Krebs-Henseleint buffer [KHB]). Immediately, assays of E_2G or CCK-8 uptake by the cells were performed in inhibitor-free KHB, as described above. CsA (Tokyo Kasei, Tokyo, Japan), which is known to have preincubation inhibition effects on the OATP1B1/1B3 function, was used as a control in any experiments relevant to the preincubation inhibition effect.

Transporter inhibition assays (long-lasting preincubation method). The long-lasting preincubation inhibition effects of DAAs on OATP1Bs were examined using a similar method to that described above. The cells were preincubated with a DAA for 30 min at 1.0 μM, after which they were washed once with inhibitor-free DMEM. Immediately thereafter, the cells were washed with KHB and then subjected to E_2G or CCK-8 uptake assays, as described above, or they were further incubated with inhibitor-free DMEM in 5% CO_2 at 37°C. After 1 or 3 h of additional incubation, the cells were washed with KHB, and the OATP1B functions were assessed by the transport assay.

Transporter inhibition assays (pre- and coincubation combination method). The cells were preincubated with DMSO (0.1%) or a DAA at concentrations of 0.1, 0.4, and 1.0 μM as described in the preincubation method, immediately after which the OATP1B functions were determined in the presence of a DAA at the same concentration used in preincubation.

Statistical analysis. Statistical analysis (Student's *t* test) was performed using a statistical software package (Statcell; OMS, Saitama, Japan) to determine whether the differences between two values were significant.

RESULTS

Validation of functional expression of OATP1B1 and OATP1B3 in HEK293 cells. Since it has been well established that the HEK293-based OATP1B expression system is useful for drug transport assessment and determining the potential for DDI, the experiments began by examining functional OATP1B expression in HEK293 cells. The results of RT-PCR and Western blotting showed that OATP1B1 mRNA and protein expression were detected exclusively in 1B1/HEK cells (Fig. 1A and B). Cell surface localization of OATP1B1 was also detected (Fig. 1C). Consistently, the results of transport assays showed that significant E_2G uptake levels were observed in 1B1/HEK cells and that this uptake was completely inhibited by RIF (Fig. 1D). Similarly, OATP1B3 mRNA and protein expression, as well as OATP1B3 cell surface localization, were detected in 1B3/HEK cells (Fig. 1E to G). As expected, BSP-sensitive CCK-8 uptake was observed in 1B3/HEK cells (Fig. 1H).

Characterization of interaction properties between OATP1B and DAAs using a coincubation inhibition method. The interaction profiles of SMV, ASV, DCV, and SFV with OATP1B1 and OATP1B3 were examined by a classical coincubation inhibition assay, where TLV was also used as a reference DAA. E_2G and CCK-8 were used as OATP1B1 and OATP1B3 substrates, respectively, because they have come to be regarded as good surrogate probes for evaluation of OATP1B-mediated DDIs (9, 23). The results showed that all DAAs tested were able to inhibit OATP1B1 function (Fig. 2); the IC_{50} values are listed in Table 2. The IC_{50} value of TLV for the OATP1B1 function was comparable to that reported in the literature (9). Compared with TLV, SMV and ASV were found to be potent inhibitors, while DCV had a similar level of inhibition and SFV was found to be a relatively weak inhibitor. Similarly, the inhibition profile of DAAs against the OATP1B3 function was also determined (Fig. 2 and Table 2). Again, the IC_{50} value of TLV for OATP1B3 was comparable to that reported in the literature (9), and other IC_{50} values showed that SMV, ASV, and DCV were all strong OATP1B3 inhibitors, while SFV did not significantly affect OATP1B3 function.

The International Transporter Consortium has proposed a decision tree for use in determining if a drug has the potential to cause OATP1B-mediated DDI (17). Using that tree, C_{max}/IC_{50} values were calculated as the initial step (Table 2). All C_{max}/IC_{50} values (except for SFV) were above the cutoff value (0.1), which suggested the need to proceed with an *R* value calculation for SMV, ASV, and DCV. It was also found that, even though they are less significant than those of TLV, the SMV *R* values for both OATP1B1 and OATP1B3 were over 1.25 (the suggested value according to the upper limit of equivalence range) (Table 2). In contrast, the *R* values of ASV and DCV were below 1.25.

Identification of preincubation inhibition effects of DAAs on OATP1B functions. Although available literature is still limited, recent evidence suggests that the preincubation inhibition effect is one of the intrinsic characteristics of OATP1B inhibitors. Therefore, we sought to clarify whether the DAAs have the capability to exert such inhibitory effects by conducting preincubation inhibition assays using CsA as a reference inhibitor. As shown in Fig. 3, preincubation with SMV at 1.0 and 10 μM results in a substantial decrease in the OATP1B1 function level by 67.7 ± 13.4% and 88.4 ± 12.9%, respectively, and a decrease in the OATP1B3 function level by 95.1 ± 3.1% and 98.1 ± 1.1%, respectively. These effects were as potent as those of CsA. Unexpectedly, the preincubation inhibition profile of ASV on OATP1B1 function was somewhat different from that of SMV, and ASV preincubation affected OATP1B3 function only at 10 μM. DCV also exhibited significant

Downloaded from http://aac.asm.org/ on July 15, 2014 by Chiba University